Coil−Globule Transition of Poly(Dimethylacrylamide): Fluorescence and Light Scattering Study

Susana Piçarra,[†,‡] Paula Relógio,[†] Carlos A. M. Afonso,[§] J. M. G. Martinho,[†] and J. P. S. Farinha*[,†]

Centro de Química-Física Molecular, Instituto Superior Técnico, 1049-001 Lisboa, Portugal, Escola Superior de Tecnologia de Setúbal, Instituto Politécnico de Setúbal, Estefanilha, 2914-508 Setúbal, Portugal, and Departamento de Química, Faculdade de Ciências e Tecnologia, Universidade Nova de Lisboa, 2829-516 Caparica, Portugal

Received May 8, 2003; Revised Manuscript Received July 31, 2003

ABSTRACT: We studied the coil−globule transition of a poly(dimethylacrylamide) (PDMA) chain (M_n = 2.5 × 10^5; M_w /M_n = 2.2) in methanol at several temperatures by steady-state and time-resolved fluorescence and by dynamic light scattering. The polymer was randomly labeled with 0.5 mol % (PDMA05Py) and 1.1 mol % (PDMA11Py) of a pyrene derivative. Temperature breakpoints in both the excimer to monomer and dimer to monomer fluorescence intensity ratios were identified with the coil−globule transition temperature T_{cg}. We obtained T_{cg} = 46 ± 7 °C for PDMA05Py (8 × 10^{-8} M in methanol) and T_{cg} = 52 ± 6 °C for PDMA11Py (3 × 10^{-8} M in methanol). Time-resolved fluorescence measurements of these solutions were analyzed using an approach based on Tashiya's model for excimer formation in micelles. Using this model we were able to calculate the polymer radii for different temperatures and identify the coil−globule transition occurring around T_{cg} = 53 ± 3 °C for PDMA05Py and about T_{cg} = 55 ± 5 °C for PDMA11Py. Finally, the hydrodynamic radii of the polymers in methanol were measured by dynamic light scattering. In these measurements we had to use more concentrated solutions (ca. 3 × 10^{-5} M in methanol) in order to detect the transition of the coiled chains. Although we also detect extensive formation of multichain aggregates at this concentration, an abrupt variation of the isolated chain radius was observed at about 50 °C for PDMA05Py and 55 °C for PDMA11Py. Both the transition temperatures and the polymer radii are in good agreement with the results obtained from the fluorescence data and, to our knowledge, provide the first evidence that the coil−globule transition detected by fluorescence techniques coincides with the transition observed in light scattering measurements.

Introduction

Coil−globule transitions have been largely studied since the sixties[1] and play an important role in several biological systems, such as DNA packing,[2] protein folding, and enzymatic activity.[3,4] The transition between the coil and globule conformations of a polymer chain depends on the properties of both solvent (molecular structure) and polymer (molecular weight and structure).[5,6] A high molecular weight polymer in a good solvent adopts a coiled configuration, as the excluded volume effect tends to extend the chain. At the θ temperature, the chain shows nearly unperturbed dimensions because the segment−solvent interactions balance the segment−segment interactions and the three body interaction terms are unimportant.[7] In a very poor solvent, the attractive segment−segment interactions will dominate over segment−solvent interactions, forcing the polymer to collapse into the globular state.[5] The transition between the coil and the globule conformations can be induced by a change in the solvent thermodynamics, for example, by changing the temperature.[8] The coil−globule transition occurs in a very small temperature interval for long stiff polymer chains but spans over a broad temperature interval for short flexible chains. Such limits have been theoretically predicted and shown by simulation.[5,9,10]

The globular state of isolated chains is not easy to detect experimentally because it is usually masked by aggregation and precipitation of the chains. To avoid this problem it is necessary to work with low molecular weight polymer chains at very low concentrations, where most of the traditionally used techniques (e.g., light scattering) are not sensitive enough. Fluorescence is a less common technique to study isolated chains in solution and detect the coil−globule transition.[11,12] However, this technique has been widely used to follow the dynamics and conformation of polymer chains in diluted solution using polymers labeled with adequate dyes,[13−18] either along the main chain,[13,18,19] on a side chain,[20] or at the chain ends.[14−16,21] Dipolar electronic energy transfer[22] between fluorescent groups (one donor and one acceptor) attached at specific sites has been used as a spectroscopic ruler to calculate distances between labeled sites in synthetic polymers[23,24] and biopolymers.[25−28] In this case the distance between dyes should remain constant on the energy transfer time scale, otherwise the measured distances would also reflect the motion of the polymer chain.[27,28] Another type of experiment uses fluorescence anisotropy measurements of labeled polymers to provide information on the segmental motion of the chain, in the nanoseconds or subnanoseconds time range.[29−31] If one is interested in the conformation and dynamics of the polymer chain instead, the time scales involved are on the order of 10 to a few hundreds of nanoseconds. Here, the formation of an excited dimer (the excimer) on the encounter of a ground-state molecule with an electronically excited molecule can also be used.[32,33] Following the time

* To whom correspondence should be addressed. E-mail: farinha@ist.utl.pt.
† Instituto Superior Técnico.
‡ Instituto Politécnico de Setúbal.
§ Universidade Nova de Lisboa.

10.1021/ma0345899 CCC: $25.00
Published on Web 09/27/2003

evolution of the excimer and monomer fluorescence of polymer chains labeled with an adequate fluorescent dye, we can calculate the rate constants relative to the approach of the labeled polymer segments.[14−16,33] From this, it is in principle possible to recover information on the dimensions of the polymer using an appropriate model. The collapse of the polymer from the coil to the globular conformation could then be detected from the change in chain dimensions. However, since this is an indirect method, it would be advantageous to compare the results obtained with another technique. This proved to be a difficult task because of the low concentrations needed in order to study the coil−globule transition without the interference of multichain aggregates. In this work we take advantage of the relatively high molecular weight of our polymer to compare the chain dimensions determined by steady-state and time-resolved fluorescence with the values obtained by dynamic light scattering. Since the concentrations used in the light scattering measurements are necessarily higher than the ones used in fluorescence (because polymer molecular weight is, however, still low for light scattering experiments), aggregation of the globules cannot be neglected.

In this paper we describe the coil−globule transition of a poly(dimethylacrylamide) (PDMA) chain ($M_n = 2.5 \times 10^5$; $M_w / M_n = 2.2$) randomly labeled with different amounts of a pyrene derivative (0.5 and 1.1 mol %) in a methanol solution, using fluorescence and light scattering techniques. Pyrene is a good dye to study the dynamics of polymers with long chains, as it is a very well characterized fluorescent dye[34,35] and has a long intrinsic fluorescent lifetime. Pyrene has been used with success to study the conformation and dynamics of chains that adopt a coil conformation more or less expanded.[33,36−40]

We start by describing the preparation of our polymers, which have exactly the same backbone and molecular weight distribution but different amounts of attached pyrene groups. These polymers were obtained from a statistical copolymer of dimethylacrylamide and *N*-(acryloxy)succinimide, poly(DMA-*st*-NAS). The reactive NAS groups can be used to incorporate different amounts of a pyrene derivative in the chain.

From steady-state fluorescence experiments we can determine the coil−globule transition temperature of the polymer. We also establish that the excimer formation rate constant is diffusion controlled, with activation energies very close to the solvent viscous flow activation energy, showing that the globules are swollen by the solvent. Loose, solvent swollen globules were also observed in other polymeric systems, especially for flexible chains with molecular weight below the critical molecular weight for entanglements, M_e.[11,41]

We analyze the time-resolved fluorescence curves with a model that considers the polymer chains divided into several blobs where pyrene groups are distributed according to a Poisson distribution.[42−44] We then present a method to calculate the dimensions of the polymer coils. The average radius calculated by this method shows a transition that agrees with the coil−globule transition temperature determined in our steady-state fluorescence experiments.

Finally we present the results obtained by dynamic light scattering, where we observe a bimodal diameter distribution. The average diameter of the larger particles (which correspond to aggregates of several chains) increases as temperature is decreased (experiments were done from higher to lower temperature) but the diameter of the smaller particles (which correspond to isolated polymer chains) remain constant down to the coil−globule transition temperature and drop to smaller values bellow it.

We conclude by comparing the results obtained by the three methods (steady-state fluorescence data, time-resolved fluorescence, and dynamic light-scattering measurements). The agreement between the results is very good, pointing to a broad coil−globule transition centered around 52 °C for the chain with higher pyrene content and around 49 °C for the chain with the lower level of labeling.

Experimental Section

Instrumentation. Fluorescence spectra were recorded on a SPEX Fluorolog F112A fluorometer at several temperatures using a cryostat from Oxford Instruments (DN 1704) that allows temperature control within ±0.5 deg. The fluorescence spectra were recorded between 370 and 600 nm using 341 and 360 nm as excitation wavelengths.

Time-resolved fluorescence intensity decays with picosecond resolution were obtained by the single-photon timing technique using laser excitation with a wavelength of 341 nm. The system consists of a mode-locked Coherent Inova 440-10 argon ion laser synchronously pumping a cavity-dumped Coherent 701-2 dye laser using DCM, which delivers 5−6 ps pulses at a repetition rate of 460 kHz. The fluorescence was observed with a polarizer at the magic angle, the scattered light being effectively eliminated by a cutoff filter. The fluorescence was selected by a Jobin-Yvon H*R*320 monochromator with a grating of 100 lines/mm and detected by a Hamamatsu 2809U-01 microchannel plate photomultiplier. To analyze the decay curves we developed software that uses a nonlinear least-squares reconvolution method based on the Marquard algorithm.[45]

Dynamic light scattering measurements were performed on a Spectra Physics model 127 He−Ne laser (632.8 nm, 35 mW) and a Brookhaven BI-2030AT autocorrelator. Time correlation functions were analyzed with a Laplace inversion program (CONTIN).

Absolute molecular weights and molecular weight distributions were determined by gel permeation chromatography (GPC), with a light scattering detector (three angles laser light scattering photometer, TALLS, Wyatt Technologies) associated to a differential refractometer detector (Waters 410). A borate buffer (50 mM, pH = 9.3) was used as eluent at a flow rate of 0.5 mL/min. The eluent was degassed (Degasser ERC-3112) before being introduced into the Waters 510 pump and the Waters Ultrahydrogel 2000 and 500 columns. Polymer solutions were prepared in borate buffer (concentration, 5 mg/mL), filtered on 0.22 μm Millex-GV PVDF filters (Durapore), and injected into a 200-μL injection loop (SSI, LP-21) connected to the pump.

Reagents and Solvents

Tetrahydrofuran, THF (99+%, Aldrich), and *tert*-butyl alcohol (>99%, Riedel-de-Haën) were dried under sodium and distilled before use. 2,2′-Azobis(isobutyronitrile), AIBN, (>98%, Fluka), was dried under vacuum and kept under nitrogen and *N*,*N*-diisopropylethylamine (1:100 in THF, Aldrich) was distilled under vacuum. *N*,*N*-Dimethylacrylamide, DMA (99% Aldrich), *N*-(acryloxy)succinimide, NAS, (>90%, Sigma), and dimethylamine (99+%, Aldrich) were used with no further purification.

Polymer Synthesis. Poly(*N,N-dimethylacrylamide-st-N-(acryloxy)succinimide), Poly(DMA-NAS).* Poly(DMA-NAS) was prepared according to a synthetic strategy that closely follows the one described by Winnik

Scheme 1

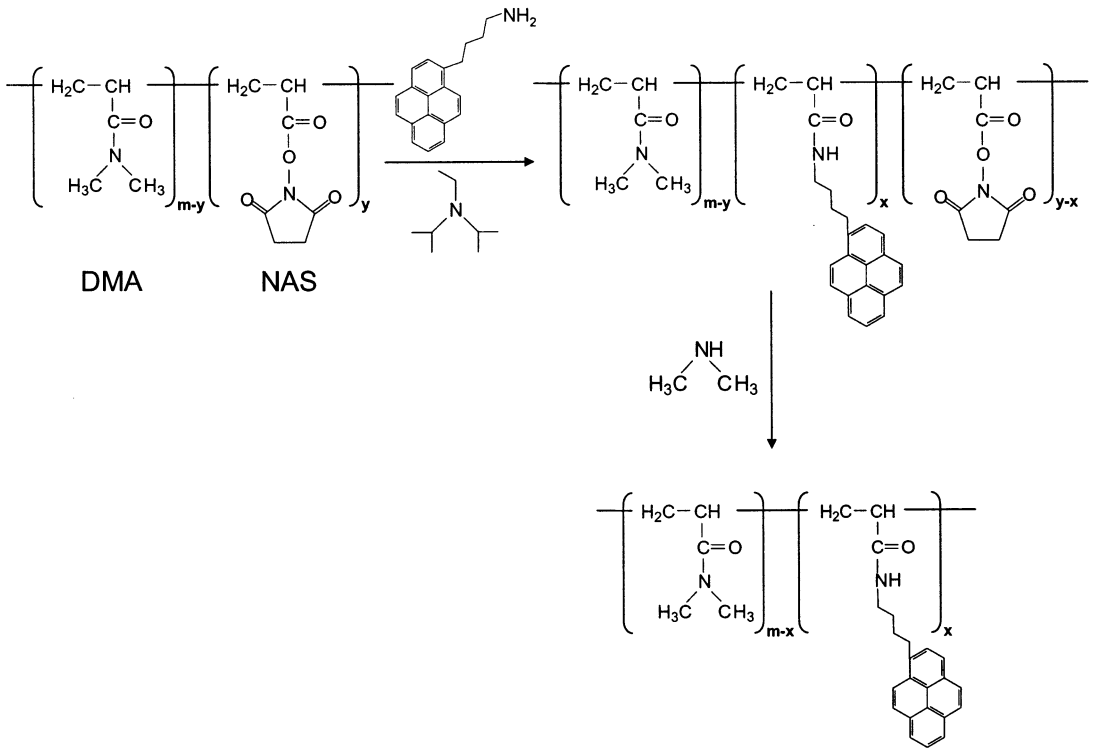

Scheme 2

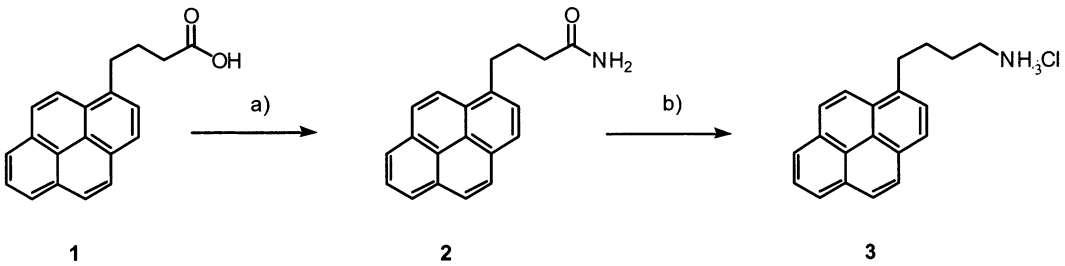

[a] (i) $(COCl)_2$ (1.05 equiv), DMF (cat), CH_2Cl_2, reflux, 1.5 h; (ii) NH_3 dry, ambient temperature, 80 %. [b] (i) $BH_3.Me_2S$ (2.5 mol equiv), distillation in THF, 97%; (ii) HCl in Et_2O.

for the preparation of the statistical copolymer poly(*N*-isopropylacrylamide-*st*-NAS).[46] *N*,*N*-Dimethylacrylamide, DMA (5.2 mL, 0.05 mol), and *N*-(acryloxy)-succinimide, NAS (0.17 g, 0.001 mol), were dissolved in *tert*-butyl alcohol (30 mL) at 70 °C under nitrogen. 2,2′-Azobis(isobutyronitrile), AIBN (30 mg), in *tert*-butanol (3 mL) was added to the solution. The reaction mixture was stirred at 70 °C for 20 h and then cooled to room temperature. The solvent was evaporated and the polymer (≈4 g) was isolated by precipitation from a THF solution into hexane.

Pyrene-Labeled PDMA. From the same poly(DMA−NAS) statistical copolymer, two labeled PDMA samples with different levels of pyrene incorporation were prepared, according to the reactions represented in Scheme 1.

The pyrenyl derivative used in these reactions is an amide, [4-(1-pyrenyl)butyl]amide,[46] which was obtained as hydrochloride (**3**), by the sequence of reactions represented in Scheme 2. The fluorescent probe was obtained from 4-(1-pyrenyl)butanoic acid (**1**), with a global yield of 78% and without any chromatographic purification. The synthesis procedure is described elsewhere.[47]

PDMA with 1.1 mol % of Pyrene (PDMA11Py). *N*,*N*-Diisopropylethylamine (0.04 mmol, 0.7 mL of a 1:100 solution in THF) was added to a solution of [4-(1-pyrenyl)butyl]amine hydrochloride (0.0124 g, 0.04 mmol) and PDMA-*co*-NAS (0.1 g) in THF (10 mL). The reaction mixture was stirred at room temperature in the dark for 24 h. Dimethylamine gas was bubbled into the reaction mixture and the solution stirred for two more hours. The polymer was isolated by precipitation in cold hexane. It was further purified by successive precipitations from a methanol solution (5 mL) at 35 °C into cold diethyl ether (50 mL) and from a THF solution into cold hexane. It was dried in a vacuum for 24 h.

PDMA with 0.5 mol % of Pyrene (PDMA05Py). The same procedure as for PDMA11Py was used. A solution of *N*,*N*-diisopropylethylamine (0.02 mmol, 0.35 mL of a 1:100 solution in THF) was added to a solution of [4-(1-pyrenyl)butyl]amine hydrochloride (0.0016 g, 0.005 mmol) and poly(DMA-*co*-NAS) (0.1 g) in THF (10 mL). The reaction mixture was stirred at room temperature in the dark for 24 h before bubbling dimethylamine gas. The reaction mixture was stirred for an additional 2-h period. A workup procedure identical with that described for PDMA11Py gave the polymer PDMA05Py.

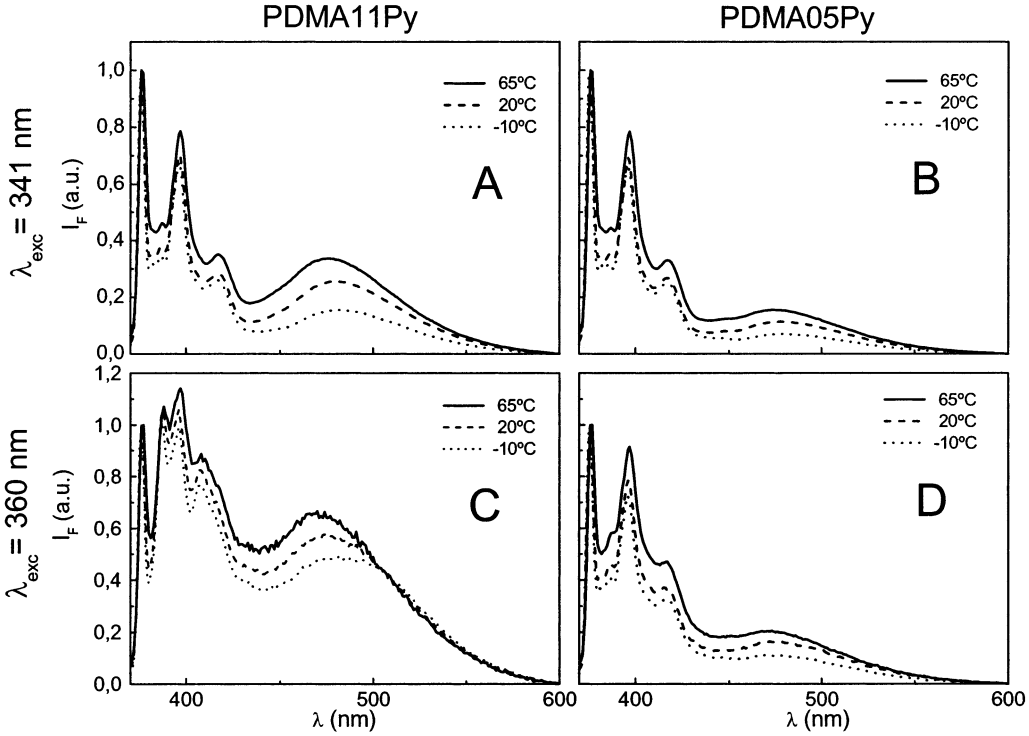

Figure 1. Normalized fluorescence emission spectra of PDMA11Py and PDMA05Py in methanol (3×10^{-8} M and 8×10^{-8} M, respectively) at −10 °C (· · ·), 20 °C (- - -), and 65 °C (——). With 341 nm excitation light (A, B), the monomer structured emission and the broad excimer emission centered around 480 nm are observed. With 360 nm excitation light (C, D) the spectra are distorted in the region around 400 nm due to dimer emission.

Polymer Characterization. The absolute molecular weights of poly(DMA-*st*-NAS) were determined by gel permeation chromatography (GPC) with universal calibration curves yielding $M_n = 251\,600$ and $M_w = 551\,900$ ($M_w/M_n = 2.2$). The purity of the polymers was assessed by gel permeation chromatography (GPC) using a scanning fluorescence detector and a refractive index detector to ascertain the absence of low molecular weight fluorescent species.

The reactivity ratio of DMA is not published, but given the structural resemblance of DMA to NAS and NAM (*N*-acryloximorpholine) and the ratios for NAM and NAS, $r_{NAS} = 0.63 \pm 0.03$ and $r_{NAM} = 0.75 \pm 0.01$,[48] we expect the copolymer of DMA and NAS to be statistical.

The final content of 4-(1-pyrenyl)butyl groups of each labeled polymer, PDMA11Py and PDMA05Py, was obtained from UV absorption data of a series of polymer solutions in methanol, using the reference [4-(1-pyrenyl)butyl]amine ($\epsilon_{342nm} = 35\,400$ dm^3 mol^{-1} cm^{-1}, determined experimentally). The samples with the highest level of pyrene incorporation (PDMA11Py) have 1.1 mol % of pyrenyl, corresponding to 27 pyrenyl groups per chain. In the second series of samples, PDMA05Py, we obtained 0.5 mol % of pyrenyl or 13 pyrenyl groups per chain. The structure of the polymer chains is represented in Scheme 1.

Sample Preparation. Fluorescence Measurements. PDMA05Py and PDMA11Py solutions (8×10^{-8} and 3×10^{-8} M, respectively) were prepared in spectroscopic grade methanol and degassed with a gentle argon flow (saturated with methanol) during 30 min. The solutions were kept in the dark at 60 °C between measurements to equilibrate in the coil conformation.

A 1.0×10^{-6} M solution of 4-(1-pyrenyl)butanoic acid (Aldrich, 97% pure, used as received) in methanol was prepared and degassed as described for the polymers.

Dynamic Light Scattering Measurements. Polymer solutions of 3×10^{-5} M were prepared in filtered spectroscopic methanol and left for 12 h at room temperature before the experiments.

Results and Discussion

Steady-State Fluorescence Measurements. The room-temperature fluorescence spectra of diluted solutions of PDMA05Py and PDMA11Py in methanol (8×10^{-8} and 3×10^{-8} M, respectively) show two separate emission bands when excited at 341 nm. One is a structured emission characteristic of the excited pyrene monomer and the other is a broad band at higher wavelengths, characteristic of the pyrene excimer. At these polymer concentrations, intermolecular excimer cannot be formed and therefore the presence of excimer emission indicates that the butylpyrene groups of the polymer come into contact.

In Figure 1 we show the normalized fluorescence spectra of PDMA05Py and PDMA11Py in methanol at −10, 20, and 65 °C. With excitation light of 341 nm (Figure 1A,B), we can detect the monomer structured emission (with maxima at 376, 396, and 430 nm) and the broad excimer emission centered around 480 nm. The change in the relative intensity of the bands at 376 and 396 nm is due to the temperature effect on the pyrene vibronic transitions and was also observed experimentally on a diluted solution of 4-(1-pyrene)-butyric acid in methanol. When excitation light of 360 nm is used (Figure 1C,D), the spectra become distorted in the region around 400 nm, indicating the presence of a new emission band.

The new band appearing at around 400 nm can be attributed to the emission of excited pyrene dimers.[49,33] Using excitation light of 360 nm the pyrene monomer has a very low molar absorption coefficient, resulting

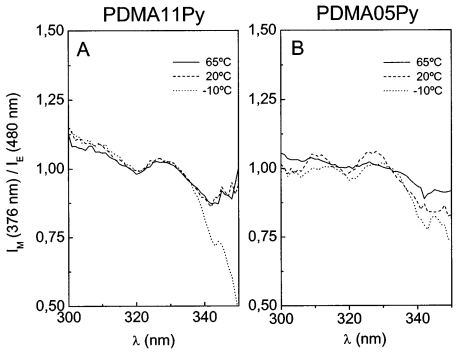

Figure 2. Ratio of emission intensities at 376 nm (monomer) and 480 nm (excimer) for PDMA11Py (A) and PDMA05Py (B) in methanol at −10 °C (· · ·), 20 °C (- - -), and 65 °C (—). The monomer-to-excimer emission ratio depends on the excitation wavelength, suggesting that the excimer state is populated both by monomer and dimer excitation.

in a higher fraction of light being absorbed by the dimers, which consequently show an increased emission. Therefore, depending on the monomer and dimer molar optical densities, the excitation light is distributed differently between these species at each wavelength. Since the dimer has its own emission and can also rearrange to form the excimer, the excitation spectra recorded at each wavelength reflect the way the emitting species are formed, showing differences as the emission wavelength is changed.

Figure 2 compares the ratio of the emission intensities at 376 nm (monomer) and 480 nm (excimer) as a function of the excitation wavelength, for the diluted solutions of PDMA05Py and PDMA11Py in methanol at −10, 20, and 65 °C. It is well-known that a concentrated solution of the model compound 4-(1-pyrene)-butyric acid follows the monomer−excimer kinetics predicted by Birks:[34,35] the ratio of monomer to excimer fluorescence intensities is constant with the excitation wavelength at a given temperature because the excimer can only be populated via the excited monomer (the excimer ground state is dissociative and there is no dimer formation). On the other hand, we found that for both PDMA05Py and PDMA11Py the monomer-to-excimer emission ratio depends only slightly on excitation wavelength. Figure 1 shows that the relative excimer emission is higher at 360 nm than at 341 nm (where the monomer optical density is higher and fraction of light absorbed by the dimer is very small). This suggests that the excimer state can also be populated by dimer excitation. From the small effect on the excitation spectra, we infer that the existence of dimers is limited and should be related to constraints imposed by the polymer chain conformation, rather than by nonrandom incorporation of the probe. This is further confirmed by the fact that, although the behavior is observed for the full range of temperatures studied, it is more pronounced for the lowest temperatures where chain constrains are more important.

Having established the existence of three excited emitting species (monomer, dimer, and excimer), the kinetics of PDMA05Py and PDMA11Py in methanol should be described by a three-states model (Scheme 3). From the three excited species, the pyrene monomer (M*), dimer (D*), and excimer (E*), only monomer (M) and dimer (D) exist in the ground state. Monomer and dimer are probably in equilibrium and upon electronic excitation can give the corresponding excited-state species, M* and D* (α being the fraction of light

Scheme 3

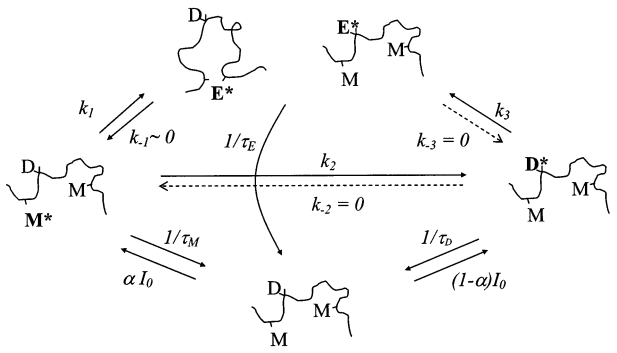

absorbed by the monomer). The ground state of the pyrene excimer is dissociative and E* cannot be produced by direct excitation. The excimer is produced either by rearrangement of D* or from the encounter of an excited monomer M* with a ground-state monomer M with a rate constant k_1. Since k_1 depends on the distance between the monomers, we have to consider a distribution of excimer formation rate constant values. D* and E* correspond to different conformations of the associated state of two pyrene moieties in the polymer chain, and, therefore, the rearrangement between D* and E* is a local process that does not involve a significant change in the polymer chain conformation. From these, E* is the most stable conformation and therefore the production of D* from E* should be unimportant at moderate temperature ($k_{-3} = 0$). Also, since D* probably rearranges rapidly to E*, we will not consider the dissociation of D* to give M and M* ($k_{-2} = 0$). Furthermore, formation of D* from the encounter of M* and M (k_2) should not be important because with 341 nm excitation (when no dimer can be directly excited) we cannot detect D*.

Once formed, the excimer can dissociate to give M and M*, with rate constant k_{-1} (this process only starts to be detectable for temperatures above 45 °C). The excited species M*, D*, and E* can decay to their corresponding ground-state species with intrinsic lifetimes τ_M, τ_D, and τ_E.

From the kinetic equations and admitting the steady−state hypothesis, we obtain for the monomer/excimer intensity ratio (k_1 represents the average value of the rate constant distribution)

$$\frac{I_E}{I_M} \propto \frac{k_1[M]}{k_{-1} + 1/\tau_E} + \frac{k_3}{k_{-1} + 1/\tau_E}\frac{[D^*]}{[M^*]} \qquad (1)$$

and for the dimer/monomer intensity ratio

$$\frac{I_D}{I_M} \propto \frac{[D^*]}{[M^*]} = \frac{k_2[M]}{k_3 + 1/\tau_D} + \frac{(1-\alpha)\{(k_1 + k_2)[M] + 1/\tau_M\}(k_{-1} + 1/\tau_E) - k_1k_{-1}[M] - \dfrac{k_{-1}k_2k_3[M]}{k_3 + 1/\tau_D}}{\alpha(k_{-1} + 1/\tau_E)(k_3 + 1/\tau_D) + (1-\alpha)k_{-1}k_3} \qquad (2)$$

In Figure 3 A,B we show the temperature dependence of the ratio of excimer to monomer emission intensities, collected at 480 and 376 nm, respectively (I_{480}/I_{376}), after excitation at 341 nm. Two different regions can be distinguished in the plots, with transitions at around 45 °C. Equivalent results were obtained for poly(ethylene oxide) in toluene[11] and poly(ϵ-caprolactone) in

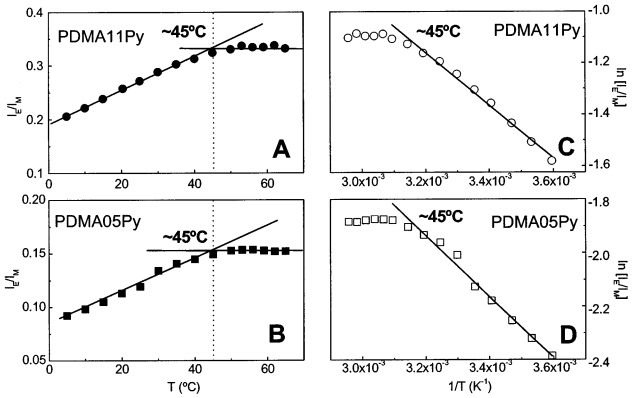

Figure 3. Temperature dependence of the ratio of excimer to monomer emission intensities I_E/I_M (collected at 480 and 376 nm, respectively, after excitation at 341 nm) for PDMA11Py (A) and PDMA05Py (B). Stevens−Ban plots of PDMA11Py (C) and PDMA05Py (D) in methanol below 45 °C (with excitation at 341 nm).

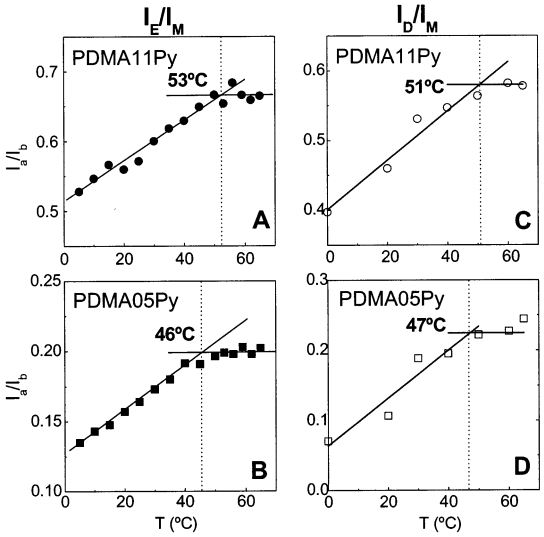

Figure 4. Temperature dependence of the emission intensity ratio of (A, B) excimer to monomerI_E(480 nm)/I_M(376 nm) and (C, D) dimer to monomer I_D(396 nm)/I_M(376 nm), for excitation at 360 nm.

tetrahydrofuran,[12] both labeled with pyrene groups at the chain ends. In those cases, two break points were found. The transition taking place at higher temperature was identified as the coil-to-globule transition: below it, polymers were in a globular state, while above they adopted a coiled conformation. The second transition, which occurred at lower temperatures, was attributed to chain aggregation followed by precipitation. This transition was not detected for the PDMA05Py and PDMA11Py.

Using 341 nm excitation light the fraction of light absorbed by the dimers is very small ($\alpha \approx 1$) and therefore [D*]/[M*] is also small. In this case eq 1 reduces to

$$\frac{I_E}{I_M} \propto \frac{k_1[M]}{k_{-1} + 1/\tau_E} \tag{3}$$

In the limit of low temperatures the excimer dissociation is not important ($k_{-1} \ll 1/\tau_E$), and since the ground-state monomer concentration [M] is approximately constant, we expect

$$\frac{I_E}{I_M} \propto \frac{k_1}{1/\tau_E} \tag{4a}$$

In this case, since τ_E is almost independent of temperature,[50] the excimer/monomer ratio will depend mainly on k_1 (the activated excimer formation process), which increases as the temperature is increased.

On the other hand, at high temperatures $k_{-1} \gg 1/\tau_E$ and

$$\frac{I_E}{I_M} \propto \frac{k_1}{k_{-1}} \tag{4b}$$

decreases with temperature since the activation energy of k_{-1} is higher than that of k_1. Therefore, the variation of I_E/I_M with temperature follows a bell-shaped curve, with a slow increase up to a maximum at the transition between the low- and the high-temperature kinetic regimes of the dye, followed by a fast decrease. Consequently, the transitions at around 45 °C observed in Figure 3 can be due either to the coil-to-globule transition and/or to the transition from the high- to the low-temperature kinetic regimes of pyrene.

From the Stevens−Ban plots[51] of PDMA05Py and PDMA11Py in methanol bellow 45 °C with excitation at 341 nm (Figure 3C,D), we calculate $E_a(k_1) = 8.9 \pm 0.7$ kJ mol^{-1} and $E_a(k_1) = 9.9 \pm 1.2$ kJ mol^{-1}, respectively. These activation energies are close to the viscosity activation energy of methanol ($E_\eta = 9.5$ kJ mol^{-1}),[52] indicating that k_1 is diffusion controlled. The dyes are therefore highly mobile, even at low temperature, feeling no constrains induced by the polymer chain conformation. This means that if a PDMA globule state is formed it is highly swelled and the ratio of excimer/monomer intensities with excitation at 341 nm is not sensitive enough to determine the coil-to-globule transition.

In Figure 4 A,B we plot the temperature dependence of the ratio of excimer to monomer emission intensities with excitation at 360 nm, collected at 480 and 376 nm, respectively, I_E(480 nm)/I_M(376 nm). In this case we observe different transition temperatures for PDMA05Py and PDMA11Py. For the less labeled chain, the transition temperature is equal for excitation wavelengths of 341 and 360 nm, but for PDMA11Py the transition temperature increases to 53 °C with 360 nm excitation. This temperature is different from the transition of the dye emission from the high- to the low-temperature region (around 45 °C in Figure 3) and can be attributed to the coil−globule transition of the chain. At this excitation wavelength the fraction of light absorbed by the dimers is higher than the fraction absorbed at 341 nm (Figure 2), and the ratio of excimer/monomer I_E/I_M must be described by eq 1. According to the results obtained with excitation at 341 nm we know that the first term in eq 1 is insensitive to the chain conformation because $E_a(k_1) \approx E_\eta$. Therefore, the change in transition temperature observed for PDMA11Py must come from the parameters in the second term of eq 1.

The temperature effect on the dimer-to-monomer ratio [D*]/[M*] can be investigated experimentally. In Figure 4C,D we show the dependence of the ratio I_D(396 nm)/I_M(376 nm) on the temperature. The dimer emission intensity was obtained by subtracting the spectra of a

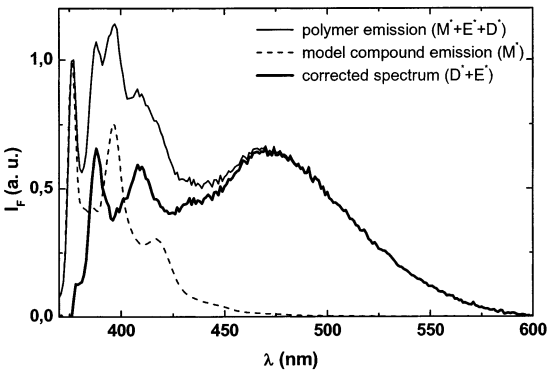

Figure 5. Correction of the emission spectra (obtained with 360 nm excitation light) of a PDMA11Py solution in methanol using 4-(1-pyrene)butyric acid as a model compound. The emission of 4-(1-pyrene)butyric acid (- - -) is subtracted from the emission of monomer, excimer and dimer (—) to give the emission spectra of the excimer and the dimer (**—**).

diluted solution of the model compound 4-(1-pyrene)-butyric acid from the emission spectra of the PDMA solutions obtained with 360 nm excitation light at each temperature, as indicated in Figure 5 for a PDMA11Py solution in methanol at 65 °C.

If there was no influence from the polymer chain, we would expect that the change in I_E/I_M with temperature was different from that of I_D/I_M, because of the difference in eqs 1 and 2 (the temperature effect on the kinetic parameters of the dye is the same but the equations are very different). However, the transitions in the I_D/I_M plot of Figure 4C,D appear at 51 ± 8 °C for PDMA11Py and 47 ± 13 °C for PDMA05Py (approximately the same temperatures as for the I_E/I_M plots, 53 ± 8 °C and 46 ± 6 °C, respectively). This suggests that we are observing conformation transitions in the polymer chains despite the change in kinetic regimes on the dye.

We can then conclude that the labeled PDMA chains show a broad coil−globule transition at around 50 °C. The globule conformation is solvent swollen, since the excimer formation process in the globule conformation is diffusion controlled. We also found that the dye content affects this temperature slightly, with an average transition about 46 ± 7 °C for the less labeled chain and 52 ± 6 °C for the chain with higher dye content.

Fluorescence Decay Curves. The fluorescence decay curves of PDMA11Py and PDMA05Py solutions in methanol (8×10^{-8} and 3×10^{-8} M, corresponding to approximately 10^{-6} M in pyrene) were measured at several temperatures from −30 to 65 °C, with excitation at 341 nm and detection set at the pyrene monomer (376 nm) and excimer (500 nm) emission wavelengths. In Figure 6 we show some of the decay curves obtained. Both PDMA11Py (Figure 6A,B) and PDMA05Py (Figure 6C,D) show decays that cannot be fitted by sums of three exponential functions. This is because the chains are randomly labeled and the excimer formation rate constant depends on the distance between pyrene groups (there is a distribution of excimer formation rate constants). The excimer decay curves (Figure 6A,C) show a well-defined initial rise time for all temperatures, suggesting that the dimer has a minor influence on the decay. This was also apparent from the steady-state results obtained with excitation at 341 nm.

To analyze the decays we followed the approach proposed by Duhamel,[42] considering that the randomly labeled chain is composed of several blobs, each with a

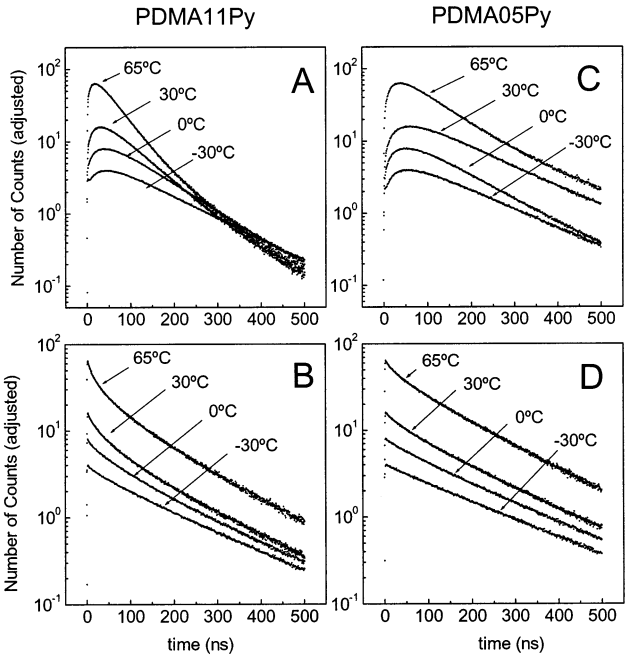

Figure 6. Fluorescence decay curves obtained for 3×10^{-6} M and 8×10^{-6} M solutions of PDMA11Py (A, B) and PDMA05Py (C, D) in methanol, with excitation at 341 nm and emission at 500 nm (A, C) and 376 nm (B, D). The decays cannot be fitted by a sum of exponential functions because the chains are randomly labeled and the excimer formation rate constant depends on the distance between pyrene groups along the chain. From the shape of the excimer decays (A, C) we conclude that the dimer has a very small influence on the overall fluorescence emission at 500 nm.

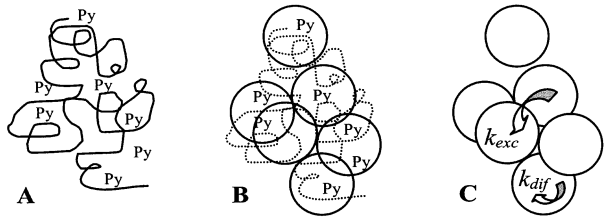

Figure 7. Cartoon of a chain randomly labeled with pyrene (A), composed of several blobs defined by the maximum distance that an excited pyrene can diffuse during its lifetime (B). Each blob has a Poisson distribution of dyes and obeys typical micelle kinetics, with ground-state pyrene groups exchanging blobs with rate constant k_{exc} and forming excimer by diffusive encounter with an excited pyrene in the same blob with rate constant k_{dif} (C).

Poisson distribution of dyes. In Figure 7 we show a cartoon of the chain divided into blobs. This is equivalent to considering that the polymer chain is composed of a number of equivalent micelles, each obeying a typical micelle model for excimer formation kinetics.[53,54]

The size of the blob is defined by the maximum distance that an excited pyrene can diffuse during its lifetime. Ground-state pyrene groups can move inside one blob and also exchange blobs with rate constant k_{exc}. Excimer formation occurs by the encounter of an excited pyrene and a ground-state pyrene in the same blob, with a diffusion controlled rate constant k_{dif}. The survival probability of the excited pyrene monomer is given by[42]

$$I_M(t) = a_1 \exp\{-(a_2 + 1/\tau_M)t - a_3[1 - \exp(a_4 t)]\} + a_5 \exp(-t/\tau_M) \quad (5)$$

where τ_M is the unquenched monomer lifetime deter-

Table 1. Monomer Intrinsic Lifetimes Determined from a Diluted Solution of the Model Compound 4-(1-Pyrene)butyric Acid in Methanol

T, °C	−30	−20	−10	0	10	20	30	55	65
τ_M, ns	243	238	233	227	225	221	204	195	192

mined using a diluted solution of the model compound 4-(1-pyrene)butyric acid in methanol (Table 1) and

$$a_2 = <n> \frac{k_{dif} k_{exc}[blobs]}{(k_{dif} + k_{exc}[blobs])^2} \quad (6)$$

$$a_3 = <n> \frac{k_{dif}^2}{(k_{dif} + k_{exc}[blobs])^2} \quad (7)$$

$$a_4 = k_{dif} + k_{exc}[blobs] \quad (8)$$

with $<n>$ being the mean number of ground-state pyrene groups in each blob and [blobs] the local concentration of blobs in the chain. The ratio $a_5/(a_1 + a_5)$ corresponds to the fraction of isolated pyrene groups, not included in any blob.

Since τ_M can be estimated independently, we analyze the experimental decay curves using five independent parameters. The model does not take into account the presence of dimers; however, using excitation at 341 nm, no dimers were detected in the steady-state fluorescence results. Another limitation of the model is that it does not allow excimer dissociation. This effect only starts to be detectable for temperatures above 45 °C.[33] However, its importance is initially very limited because it mainly affects the early decay times, which have a small weight in the fluorescence decay curve. To include excimer dissociation in the model, the (already large) number of adjustable parameters should be increased. Instead, we chose to start the fitting of the decays taken at temperatures above 45 °C a few nanoseconds after the maximum of the monomer decay.

From the values of the parameters a_2, a_3, and a_4 we determine $<n>$, k_{exc} [blobs], and k_{dif}

$$<n> = \frac{(a_2 + a_3)^2}{a_3} \quad (9)$$

$$k_{exc}[blobs] = \frac{a_2 a_4}{a_2 + a_3} \quad (10)$$

$$k_{dif} = \frac{a_3 a_4}{a_2 + a_3} \quad (11)$$

To analyze the experimental monomer decays (emission wavelength 376 nm), we developed software that uses a nonlinear least-squares method based on the Marquard algorithm[45] to compare the experimental fluorescence decays with the curves obtained by convoluting eq 5 with the experimental instrument response functions $L(t)$:

$$I_M^{conv}(t) = \int_0^t L(s) I_M(t - s)\, ds \quad (12)$$

In all of the fittings we got reduced χ^2 under 1.1 and well-distributed weighted residuals and autocorrelation of the residuals.

The fraction of isolated pyrene groups in PDMA11Py and PDMA05Py that do not participate in blobs is very small, $a_5/(a_1 + a_5) = 0.009 \pm 0.005$, over the full range of temperatures.

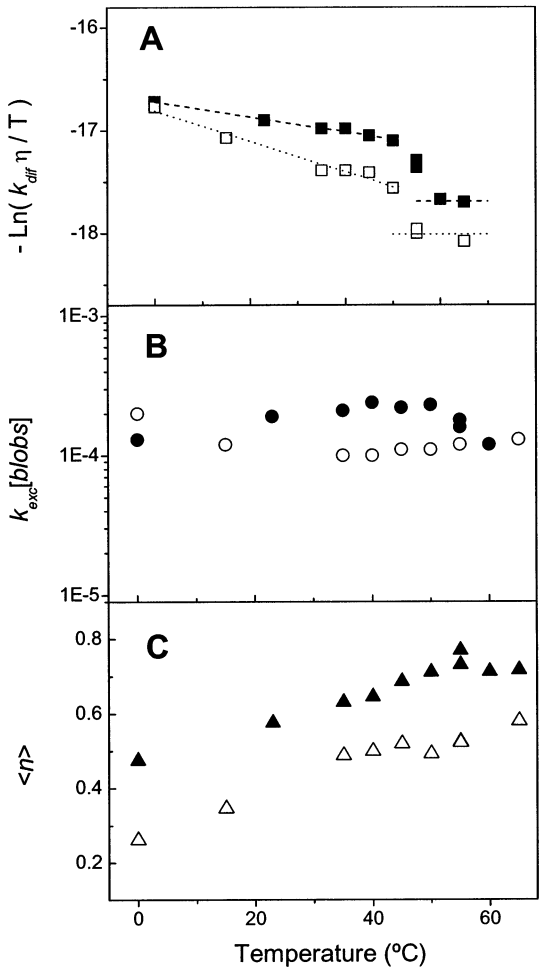

Figure 8. (A) Rate constants for excimer formation k_{dif} corrected for the effect of solvent viscosity, (B) rate constants for the exchange of pyrene between blobs k_{exc} [blobs], and (C) mean number of ground-state pyrene groups in each blob $<n>$. Values for PDMA11Py are represented in *solid* symbols and for PDMA05Py in *open* symbols.

In Figure 8A we observe that the excimer formation rate constant corrected for the effect of viscosity $k_{dif}\eta/T$ decreases with the temperature increase up to 50 °C. This is because $k_{dif}\eta/T$ is inversely proportional to the blob volume (cf. eq 13 bellow) and the volume probed by the pyrene groups (defined as the blob volume) increases with temperature. After that, there is a transition that corresponds to a large change in blob volume, which we relate to the coil−globule transition. The rate constant of pyrene exchange between blobs k_{exc}[blobs] is not very dependent on temperature (Figure 8B) but the mean number of ground-state pyrene groups in each blob $<n>$ increases with the temperature (Figure 8C), apparently indicating that the number of blobs decreases.

The rate constant of excimer formation in a blob, k_{dif}, is related to the volume of the blob, V_{blob}, because this volume defines the maximum span of the monomer diffusion during the lifetime of the excited monomer in the blob[55,56]

$$k_{dif} = \frac{2}{3} \frac{k_B T}{\eta V_{blob}} \quad (13)$$

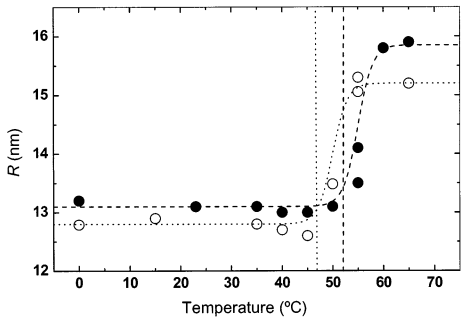

Figure 9. Plot of the polymer chain radius calculated from eq 14 vs temperature for PDMA11Py (●) and for PDMA05Py (○). The transition is centered around 55 ± 5 °C for PDMA11Py and around 53 ± 3 °C for PDMA05Py. The fitted curves are shown only as a guide. Vertical lines correspond to the mean value of the transition obtained from the steady-state results.

where k_B is the Boltzman constant, T the temperature, and η the viscosity. Since the number of blobs in a chain, $N_{blobs} = n_{Py}/<n>$, is given by the ratio of the number of ground-state pyrene groups per chain n_{Py} and the mean number of ground-state pyrene groups in each blob $<n>$, the volume of the polymer chain equals the product of the blob volume and the number of blobs per chain, $V_{chain} = N_{blobs}V_{blob}$. The radius of the polymer chain is then given by

$$R_{chain} = \left(\frac{n_{Py}k_BT}{2\pi <n> \eta k_{dif}}\right)^{1/3} \qquad (14)$$

We calculated the radius of the polymer chain using the values of $<n>$ obtained from fitting the experimental decay curves, the viscosity of methanol,[52] and the number of pyrene groups per chain n_{Py} determined by UV absorption (27 for PDMA11Py and 13 for PDMA05Py). In Figure 9 we plot the radius of the polymer chain calculated from eq 14. A transition is apparent for both polymers: in the PDMA11Py solution it is centered at around 55 ± 5 °C and for PDMA05Py at 53 ± 3 °C. This agrees fairly well with the steady-state data, where transitions centered at about 52 ± 6 °C for the chain with higher dye content and 46 ± 7 °C for the less labeled chain were detected.

Dynamic Light Scattering Measurements. To detect the globule state of isolated chains it is necessary to work at very low concentrations, so that we can avoid the formation of multiple chain aggregates which mask the coil−globule transition. However, the light scattering technique is not sensitive enough to measure solutions of a polymer with molecular weight as low as 250K at concentrations as diluted as those used in the fluorescence studies. To obtain good signal-to-noise ratios with the available laser power, we had to use 3 × 10^{-5} M solutions of PDMA11Py and PDMA05Py in methanol, which were about 3 orders of magnitude higher than the ones used for fluorescence experiments. The solutions were prepared 12 h before the measurements and allowed to rest at room temperature so that, in case phase separation occurs, the aggregates would be large enough to be easily distinguishable from the isolated chains. Measurements were preformed from 63 °C down to 40 °C, with stabilization times of at least 30 min after each temperature change. The CONTIN method[57] was used in the analysis of the correlation curves.

In Figure 10A we present the diameter distribution obtained for the solution of PDMA05Py at 54 °C. The

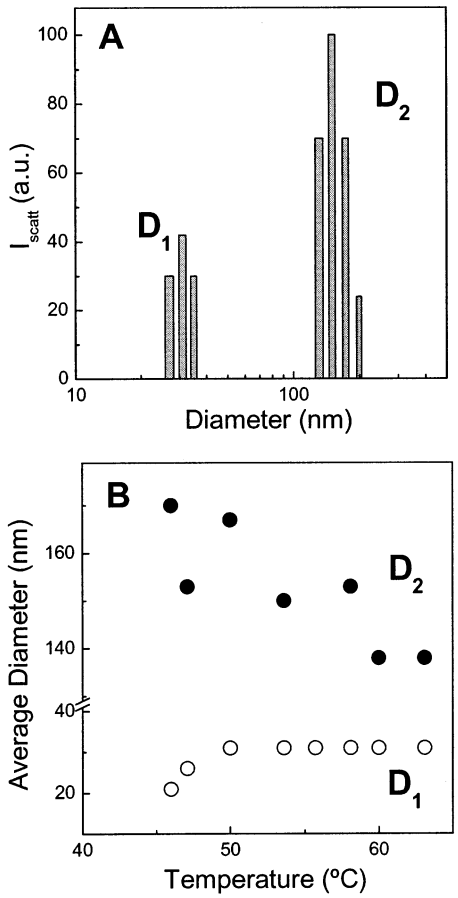

Figure 10. Diameter distribution obtained for the solution of PDMA05Py in methanol at 54 °C. The distribution is bimodal, centered at $D_1 = 31$ nm and $D_2 = 150$ nm (A). The average diameter D_2 increases as the temperature is decreased (experiments were done from higher to lower temperature), but the average diameter of the smaller particles D_1 is constant from 63 to 50 °C (corresponding to a 10-h time interval) and decreases below this temperature (B).

distribution is bimodal, with maxima centered at $D_1 = 31$ nm and $D_2 = 150$ nm. This bimodal distribution was obtained for all the tested temperatures, with the average diameters D_1 and D_2 changing with the temperature (Figure 10B). However, while the values of D_2 increase as we decrease the temperature (experiments were done from higher to lower temperature), the values of the smaller particles D_1 were constant from 63 to 50 °C (corresponding to a 10-h time interval), dropping to lower values below this temperature.

The distribution centered in D_2 corresponds to multichain aggregates that were formed because the concentration used in these experiments is much larger than the concentration used in the fluorescence measurements. The hydrodynamic radius of the aggregates increases from about 125 to 175 nm, because demixing evolutes in time[58] and the decrease in temperature enhances the demixing kinetics.[59,60]

The behavior of the distribution of the smaller sized particles corresponds to isolated polymer chains and is similar for PDMA11Py and PDMA05Py (Figure 11). For PDMA11Py the mean hydrodynamic radius of the chains is constant from 63 to 56 °C ($R_h = 15.5$ nm) and decreases to $R_h = 14.0$ nm at 55.2 °C. Bellow 53.6 °C we cannot detect any signal for individual chains, not only because of the reduced size of the chains in the globular conformation, but also because of their very low

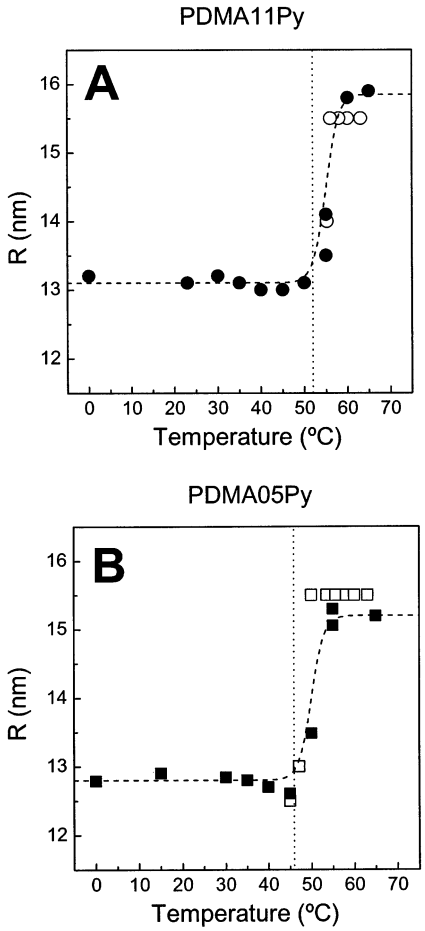

Figure 11. Hydrodynamic radius of isolated polymer chains determined by dynamic light scattering (*open* symbols) of PDMA11Py (A) is constant above 56 °C (R_h = 15.5 nm), decreasing at 55.2 °C. For PDMA05Py (B) the average hydrodynamic radius is R_h = 15.5 nm for temperatures above 50 °C. This values drops to R_h = 13.0 nm at T = 47 °C. The chain radius calculated from the time-resolved fluorescence results (*solid* symbols) for PDMA11Py (A) and PDMA05Py (B) agrees very well with the results obtained by light scattering. The two techniques point to a coil−globule transition around 55 °C for PDMA11Py and 50 °C for PDMA05Py. The fitted curves and vertical lines shown have the same meaning as those of Figure 9.

number density (as a result of the extensive aggregation). The PDMA05Py polymer has a mean hydrodynamic radius of R_h = 15.5 nm for temperatures above 50 °C. This value lowers to R_h = 13.0 nm at T = 47 °C and becomes impossible to be measured bellow 45 °C (again because of the extensive aggregation). These results also indicate that dynamic light scattering measurements could not detect any representative change in the hydrodynamic radii of the polymer coils due to the different degree of labeling of PDMA05Py and PDMA11Py.

The chain radii calculated from the time-resolved fluorescence results are also plotted in Figure 11. The agreement between the results of the two techniques is very good: for PDMA11Py both the chain radius determined by fluorescence and the hydrodynamic radius point to a coil−globule transition around 55 °C, in agreement with the steady-state fluorescence results, which pointed to a transition centered at 52 ± 6 °C. The PDMA05Py chain shows a coil−globule transition starting between 45 and 50 °C, coinciding with the time-resolved fluorescence results, which pointed to a transition around 53 ± 3 °C, and the steady-state fluorescence where we found a transition centered at about 46 ± 7 °C. We think that the good agreement between the absolute values of the hydrodynamic radii and the radii determined by fluorescence might be a coincidence. Further studies are necessary to clarify the relation between these values.

The laser used in the light scattering instrument had too low power to conduct the measurements at temperatures bellow the coil−globule transition (where very low concentrations of isolated chains are present due to chain aggregation). Nevertheless, we found a reasonable agreement between the light scattering results and the ones obtained by fluorescence techniques. This result is very important because, to our knowledge, it is the first time that both types of techniques have been used to characterize the coil−globule transition in the same polymer system. This allowed us to prove that the information obtained from both techniques is in good agreement and therefore validate the fluorescence results obtained for transitions in smaller polymer chains that cannot be detected by light scattering.[11,12]

Another important feature of our results is that, for all the used techniques, the coil−globule transition temperatures depends only slightly on the dye content of the polymers, the less labeled polymer showing a lower transition temperature. Since the coil−globule transition is expected to be broad (because the polymer molecular weight distribution is also broad), the average difference of 3 °C observed between the coil−globule transition temperatures of PDMA05Py and PDMA11Py is negligible.

Conclusions

The coil−globule transition of two PDMA chains with exactly the same molecular weight distribution, but randomly labeled with different amounts of a pyrene derivative (1.1% for PDMA11Py and 0.5% for PDMA05Py), was studied both by fluorescence and light scattering techniques.

The fluorescence experiments were done using very diluted polymer solutions (about 10^{-8} M) in methanol, for which no aggregation was detected. The coil−globule transition temperatures were determined from both steady-state and time-resolved fluorescence data. In the first case, the transition temperatures corresponded to breakpoints in both excimer-to-monomer and dimer-to-monomer intensity ratio plots. We obtained T_{cg} = 46 ± 7 °C for PDMA05Py and T_{cg} = 52 ± 6 °C for PDMA11Py. We also learned that the PDMA globule is highly swelled because the excimer formation process is diffusion controlled. Analysis of the monomer fluorescence decays allowed us to calculate the chain radii for different temperatures. Here, the changes in polymer radius, occurring around T_{cg} = 55± 5 °C for PDMA11Py and T_{cg} = 53± 3 °C for PDMA05Py, were identified with the coil−globule transition.

Dynamic light scattering measurements in 3 × 10^{-5} M polymer solutions in methanol yielded transitions around 55 and 50 °C for PDMA11Py and PDMA05Py. Unfortunately, the occurrence of aggregation on the light scattering experiments (due to the higher polymer concentration necessary to detect the transition) did not allow us to determine the radii of the globules. These results are, however, in reasonable agreement with the transition temperatures obtained from the fluorescence data, providing evidence that the coil−globule transition

detected by fluorescence techniques coincide with the transition observed in light-scattering measurements. This result is of extreme importance, since it allows the extension of coil−globule transition studies to systems of low molecular weight polymers in diluted solutions (usually bellow the light scattering limit of detection), for which the globules can be studied with no interference from multichain aggregates.

Due to the relatively broad molecular weight distribution of the polymer ($M_w/M_n = 2.2$) we expected a broad coil−globule transition. This is indeed the case for the fluorescence results, but the light scattering data show a much sharper transition. We think that the apparently abrupt transition detected in light-scattering measurements is related to the large uncertainties in our hydrodynamic radii: in order to minimize the effect of aggregation, while still detecting the isolated polymer chains, we had to use concentrations close to the detection limit of our light-scattering system.

The present results also point to a very small influence of the degree of pyrene labeling on the coil−globule transition. We found an average difference of only 3 °C between the midpoints of the transition zones for PDMA11Py and PDMA05Py. This is very small when compared to the broad transition observed for this polymer.

Acknowledgment. We thank Dr. A. Fedorov for the setting of the laser time-resolved fluorescence equipment, Dr. M. -T. Charreyre (CNRS-BioMerrieux, Lyon) for access to the GPC equipment, and FCT for financial support through project POCTI/P/QUI/14057. Susana Piçarra and Paula Relógio acknowledge FCT for PhD grants GPXXI/BD/2979/96 and SFRH/BD/1224/2000.

References and Notes

(1) Stockmayer, W. H. *Macromol. Chem. Phys.* **1960**, *35*, 54.
(2) Takahashi, M.; Yoshikawa, K.; Vasilevskaya, V. V.; Khokhlov, A. R. *J. Phys. Chem. B* **1997**, *101*, 9396.
(3) Doniach, S.; Garel, T.; Orland, H. *J. Phys. Chem.* **1996**, *100*, 1601.
(4) Chan, H. S.; Dill, K. A. *Phys. Today* **1993**, 24.
(5) Grosberg, A. Yu.; Khokhlov, A. R. *Statistical Physics of Macromolecules* AIP Press: New York, 1994.
(6) Doye; J. P. K.; Sear, R. P.; Frenkel, D. *J. Chem. Phys.* **1998**, *108*, 2134.
(7) Doi, M.; Edwards, S. F. *The Theory of Polymer Dynamics*; Oxford University Press: Oxford, 1986.
(8) Flory, P. J. *J. Chem. Phys.* **1949**, *17*, 303.
(9) Raos, G.; Allegra, G. *J. Chem. Phys.* **1997**, *107*, 6479.
(10) Hu, W. *J. Chem. Phys.* **1998**, *109*, 3686.
(11) Farinha, J. P. S.; Piçarra, S.; Miesel, K.; Martinho, J. M. G. *J. Phys. Chem. B* **2001**, *105*, 10536.
(12) Piçarra, S.; Gomes, P. T.; Martinho, J. M. G. *Macromolecules* **2000**, *33*, 3947.
(13) Monnerie, L. In *Photophysical and Photochemical Tools in Polymer Science*; Winnik, M. A., Ed.; D. Reidel: Dordrecht, The Netherlands, 1985.
(14) Winnik, M. A. *Acc. Chem. Res.* **1985**, *18*, 73.
(15) Winnik, M. A. in *Photophysical and Photochemical Tools in Polymer Science*; NATO ASI Series, Vol. 182; Winnik, M. A., Ed.; Reidel: Dordrecht, 1986.
(16) Winnik, M. A.; Redpath, A. E. C.; Paton, K.; Danhelka, J. *Polymer* **1984**, *25*, 91.
(17) Morawetz, H. *J. Lumin.* **1989**, *43*, 59.
(18) Moffitt, M.; Farinha, J. P. S.; Winnik, M. A.; Rohr, U.; Mullen, K. *Macromolecules* **1999**, *32*, 4895.
(19) Horinaka, J.; Ito, S.; Yamamoto, M.; Tsujii, Y.; Matsuda, T. *Macromolecules* **1999**, *32*, 1134.
(20) Kitamura, S. Yunokawa, H.; Kuge, T. *Polym. J.* **1982**, *14*, 85.
(21) Horinaka, J.; Maruta, M.; Ito, S.; Yamamoto, M. *Macromolecules*, **1999**, *32*, 2270.
(22) Förster, Th. *Ann. Phys.* **1948**, *2*, 55.
(23) Liu, G.; Guillet, J. E. *Macromolecules* **1990**, *23*, 1393.
(24) Liu, G.; Guillet, J. E.; Al-Takrity, E. T. B.; Jenkins, A. D.; Walton, D. R. M. *Macromolecules* **1991**, *24*, 68.
(25) Dos Remedios, C. G.; Moens, P. D. *J. Struct. Biol.* **1995**, *115*, 175.
(26) Wu. P.; Brand, L. *Anal. Biochem.* **1994**, *218*, 1.
(27) Haas, E.; Katchalski-Katzir, E.; Seinberg, I. Z. *Biopolymers* **1978**, *17*, 11.
(28) Lakowicz, J. R.; Kusba, J.; Wiczk, W.; Gryczynski, I.; Johnson, M. L. *Chem. Phys. Lett.* **1990**, *173*, 319.
(29) Monnerie, L. In *Photophysical and Photochemical Tools in Polymer Science*; Winnik, M. A., Ed.; D. Reidel: Dordrecht, The Netherlands, **1985**.
(30) Horinaka, J., Maruta, M.; Ito, S.; Yamamoto, M. *Macromolecules* **1999**, *32*, 1134.
(31) Horinaka, J.; Ito, S.; Yamamoto; M.; Tsujii, Y.; Matsuda, T. *Macromolecules* **1999**, *32*, 2270.
(32) Cuniberti, C.; Perico, A. *Eur. Polym. J.* **1977**, *13*, 369.
(33) Farinha, J. P. S.; Martinho, J. M. G.; Xu, H.; Winnik, M. A.; Quirk, R. P. *J. Polym. Science., Polym. Phys.* **1994**, *32*, 1635.
(34) Birks, J. B. *Photophysics of Aromatic Molecules*; Wiley-Interscience: London, 1970.
(35) Birks, J. B. *Rep. Prog. Phys.* **1975**, *38*, 903.
(36) Winnik, M. A.; Redpath, A. E. C. *J. Am. Chem. Soc.* **1980**, *102*, 6869.
(37) Martinho, J. M. G.; Martinho, M. H.; Winnik, M. A.; Beinert, G. *Makromol. Chem. Suppl.* **1989**, *15*, 113.
(38) Martinho, J. M. G.; Winnik, M. A. *Macromolecules* **1986**, *19*, 2281.
(39) Martinho, J. M. G.; Reis e Sousa, A. T.; Winnik, M. A. *Macromolecules* **1993**, *26*, 4484.
(40) Redpath, A. E. C.; Winnik, M. A. *J. Am. Chem. Soc.* **1982**, *104*, 5604.
(41) Yu, J.; Wang, Z.; Chu, B. *Macromolecules* **1992**, *25*, 1618.
(42) Mathew, A. K.; Siu, H.; Duhamel, J. *Macromolecules* **1999**, *32*, 7100.
(43) Kanagalingam, S.; Ngan, C. F.; Duhamel, J. *Macromolecules* **2002**, *35*, 8560.
(44) Kanagalingam, S.; Spartalis, J.; Cao, T.-M.; Duhamel, J. *Macromolecules* **2002**, *35*, 8571.
(45) Marquardt, D. W. *J. Soc. Ind. Appl. Math.* **1963**, *11*, 431.
(46) Winnik, F. M. *Macromolecules* **1990**, *23*, 242.
(47) Afonso, C. A. M.; Farinha, J. P. S. *J. Chem. Res. (S)* **2003**, *41*, 637.
(48) D'Agosto, F.; Charreyre, M.-T.; Veron, L.; Lauro, M.-F.; Pichot, C. *Macrom. Chem. Phys.* **2001**, *202*, 1689.
(49) Winnik, F. M. *Chem. Rev.* **1993**, *93*, 587.
(50) Martinho, J. M. G.; Farinha, J. P. S.; Berberan-Santos, M. N.; Duhamel, J.; Winnik, M. A. *J. Chem. Phys.* **1992**, *96*, 8143.
(51) Stevens, B.; Ban, M. I. *Trans. Faraday Soc.* **1964**, *60*, 1515.
(52) Perry, R. H.; Green, D. H *Chemical Engineers' Handbook*, 7th ed.; McGraw-Hill: New York, 1997.
(53) Infelta, P. P.; Gratzel, M.; Thomas, J. K. *J. Phys. Chem.* **1974**, *78*, 190.
(54) Tashiya, M. *Chem. Phys. Lett.* **1975**, *33*, 289.
(55) Cuniberti, C.; Perico, A. *Prog. Polym. Sci.* **1984**, *10*, 271.
(56) Lee, S.; Duhamel, J. *Macromolecules* **1998**, *31*, 9193.
(57) Provencher, S. W. *Comput. Phys. Commun.* **1982**, *27*, 213.
(58) Binder, K.; Stauffer, D. *Phys. Rev. Lett.* **1974**, *33*, 1006.
(59) Graham, P. D.; McHugh, A. J. *Macromolecules* **1998**, *31*, 2565.
(60) Piçarra, S.; Pereira, E. J. N.; Bodunov, E. N.; Martinho, J. M. G. *Macromolecules* **2002**, *35*, 6397.

MA0345899